POLITECNICO DI TORINO
Repository ISTITUZIONALE

A Complete Noise- and Scattering-Parameters Test-Set

(Article begins on next page)

05 August 2020

A Complete Noise- and Scattering-Parameters Test-Set

Marco Garelli, *Member, IEEE*, Andrea Ferrero, *Senior Member, IEEE*, and Serena Bonino

Abstract—We present an innovative test-set based on a microwave tuner, a vector network analyzer and a Y-factor receiver capable of extracting the noise and the scattering parameters of a two-port device. To the authors' knowledge, the presented test-set is the first noise system that avoids the use of any microwave switch in the noise measurement branches. A set of reflectometers and a novel calibration scheme are used to measure the tuner's loss and S-parameters in real time without any tuner precharacterization.

Index Terms—Amplifier measurement, multiport scattering calibration, noise figure, noise parameters, scattering calibration, unknown thru.

I. INTRODUCTION

THE ACCURATE measurement of amplifier and transistor noise parameters, i.e., the minimum noise temperature $T_{\min}$, the optimum source reflection coefficient Γ_{opt}, and the noise resistance R_n [1] is a challenging problem due to the multitude of terms affecting the results.

The knowledge of the device-under-test (DUT) scattering parameters, as well as the source reflection coefficients, are fundamental to estimate the proper input/output noise levels and were typically obtained by a vector network analyzer (VNA) connected to the DUT and tuner ports in different ways by electromechanical switches [2]–[6]. However, the use of microwave switches reduces the overall accuracy both by adding extra losses and by introducing a repeatability error.

Since the calibrated noise source sets the reference noise temperatures, the losses up to the DUT input should be measured and deembedded [7]. This step is also required during the noise receiver calibration.

Simpler systems use the VNA to independently precharacterize the source tuner losses, thus a tradeoff between speed and characterization points has to be made. Furthermore, the measurement is affected by the tuner mechanical repeatability [8], [9].

In this paper, we present an innovative test-set based on the Y-factor method, which avoids electromechanical switches in the main path, measures the tuner and DUT S-parameters in real time, and carefully estimates the connection losses up to the DUT reference planes with an innovative vectorial noise scattering calibration. Moreover, we do not assume the equivalence of the cold and hot noise source reflection coefficients in the computation [10].

II. SYSTEM DESCRIPTION

The measurement system is drawn in Fig. 1 on the following page. Its complexity arises from the need to measure the DUT S-parameters *and* the losses between the noise source and the DUT input.

The three reflectometers R1, R2, and R3 are used in turn to sample the incident and reflected waves at the DUT ports (planes P1 and P2) and at the external ports (P3 and P4). Four directional couplers (C1, C2, C3, and C4) feed the system with the RF excitation signal through the single-pole four-throw (SP4T) switch SW2. The VNA then measures the six outputs of the reflectometers by means of the single-pole six-throw (SP6T) p-i-n diode switch SW1, all referenced to the same signal. Finally, a microwave passive tuner is used to synthesize different source reflection coefficients at the DUT input port (plane P1).

During the DUT scattering parameters measurement only reflectometers R1 and R2 are used, being the RF drive signal sent through C1 or C2, as seen in Fig. 2.

The tuner section S-matrix from plane P3 (noise source) to plane P1 (DUT input) is measured by the R3 and R1 reflectometers with signal drive through couplers C3 or C1 (Fig. 3).

The noise capability is based on the Y-factor measurement technique. The calibrated noise source is regularly switched on (hot state) and off (cold state). It generates known noise powers into the tuner section, which reach the DUT input port at P1, but are affected by attenuation and thermal noise along the path (Fig. 4).

Since the tuner section losses can be measured for each tuner position by its S-matrix, the noise powers incident into the DUT input port can be accurately computed, based on the noise source excess noise ratio (ENR) table.

The DUT output noise power is amplified by a high-gain low-noise amplifier (LNA) and fed to the Y-factor receiver built by a spectrum analyzer that measures the hot and cold average noise levels.

III. SCATTERING PARAMETERS CAPABILITY

The test-set is a multiport environment with three main ports: P1, P2, and P3. The fourth port (P4) is used during the scattering parameter calibration, but not used in the scattering and noise measurements. As will be clarified, the calibration takes advantage of this auxiliary port to improve the measurement accuracy of the tuner section losses.

A. Calibration Model

Each port i $(i = 1, 2, 3, 4)$ is uniquely associated with its own set of error coefficients that link the sampled waves from
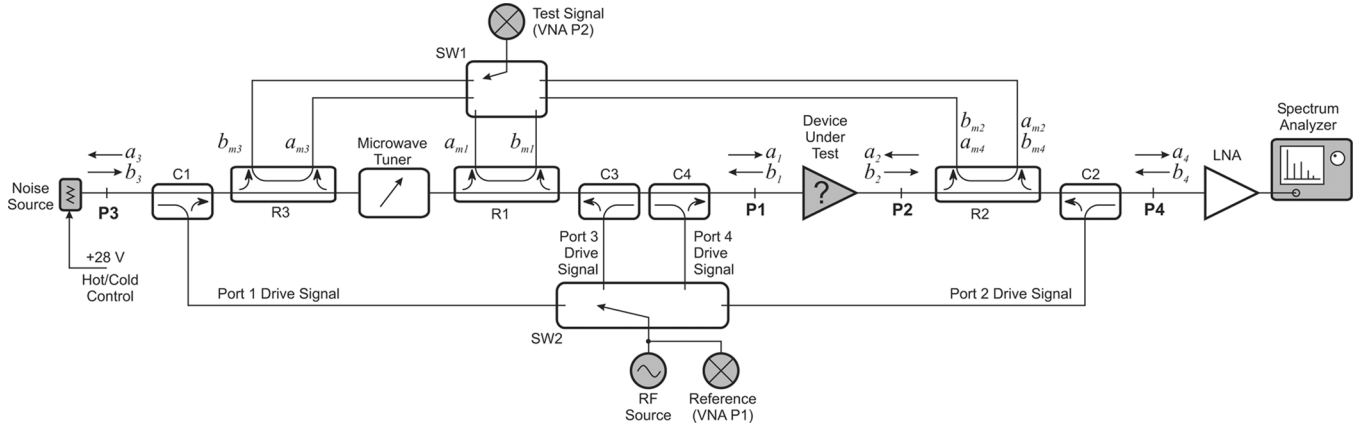
Fig. 1.   Proposed noise- and scattering-parameters test-set. The VNA is an Anritsu MS4623B, the noise source is a Noise/COM NC346B, and the spectrum analyzer is an HP8563E.
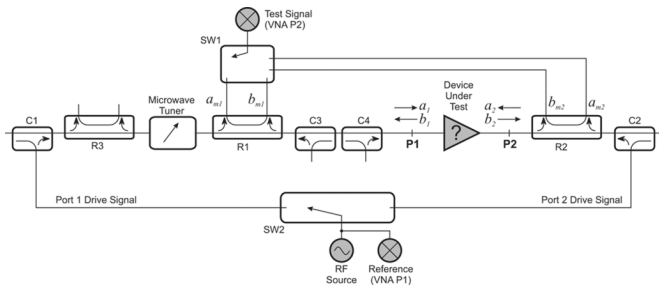

Fig. 2.   Main signal paths for the DUT S-parameters measurement. The schematic is a reduction of Fig. 1; for clarity, unused connections are not drawn.
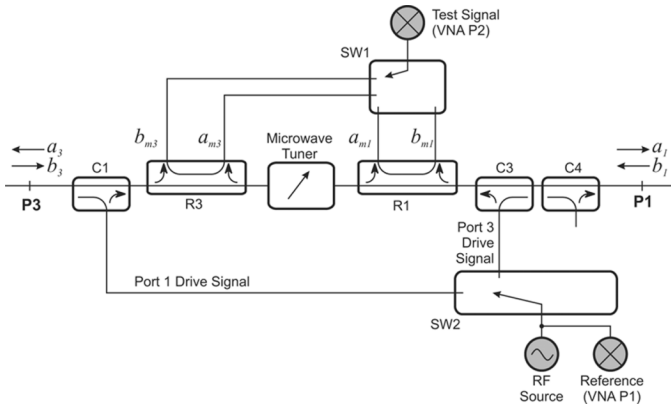

Fig. 3.   Main signal paths for the tuner section measurement. The schematic is a reduction of Fig. 1; for clarity, unused connections are not drawn.
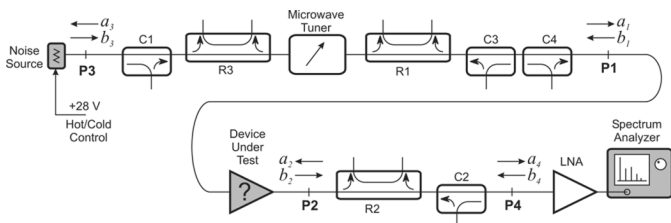

Fig. 4.   Main signal paths for the DUT noise parameters measurement. The schematic is a reduction of Fig. 1; for clarity, unused connections are not drawn.

the reflectometers to the actual incident and reflected waves at the port plane (as in [11, eq. (1)])

$$a_i = l_i b_{mi} - h_i a_{mi}$$
$$b_i = k_i b_{mi} - m_i a_{mi} \qquad (1)$$

where a_i and a_{mi} are the actual and measured incident waves at port i, b_i and b_{mi} are the actual and measured reflected waves, and in the following, we will use the ith port error coefficients organized in the error matrix:

$$\boldsymbol{E}_i = \begin{bmatrix} -h_i & l_i \\ -m_i & k_i \end{bmatrix} = k_i \begin{bmatrix} \dfrac{-h_i}{k_i} & \dfrac{l_i}{k_i} \\ \dfrac{-m_i}{k_i} & 1 \end{bmatrix}. \qquad (2)$$

Being that this error model a generalization of the eight-term error model, it is well known that in a n-port VNA without leakage, the error terms are $4n - 1$ since one term is free [12]. Our choice is to normalize all the error coefficients by k_1.

Thus, the scattering parameter calibration involves 15 terms, and it is performed in three steps: the first two solve for seven unknowns each, and the last one computes the remaining term.

Step One. A two-port calibration[1] is made at planes P1 and P2 (Fig. 5).

The calibration computes the $\boldsymbol{E}_1/k_1$ and $\boldsymbol{E}_2/k_1$ error matrices as

$$\boldsymbol{E}_1/k_1 = \begin{bmatrix} \dfrac{-h_1}{k_1} & \dfrac{l_1}{k_1} \\ \dfrac{-m_1}{k_1} & 1 \end{bmatrix} \quad \boldsymbol{E}_2/k_1 = \begin{bmatrix} \dfrac{-h_2}{k_1} & \dfrac{l_2}{k_1} \\ \dfrac{-m_2}{k_1} & \dfrac{k_2}{k_1} \end{bmatrix} \qquad (3)$$

so seven error coefficients l_1/k_1, m_1/k_1, and h_1/k_1 and l_2/k_1, m_2/k_1, h_2/k_1, and k_2/k_1 are determined.

Step Two. A second two-port calibration is performed at planes P3 and P4 (Fig. 6) with a thru device between P1 and P2.

This calibration computes the $\boldsymbol{E}_3/k_3$ and $\boldsymbol{E}_4/k_3$ error matrices

$$\boldsymbol{E}_3/k_3 = \begin{bmatrix} \dfrac{-h_3}{k_3} & \dfrac{l_3}{k_3} \\ \dfrac{-m_3}{k_3} & 1 \end{bmatrix} \quad \boldsymbol{E}_4/k_3 = \begin{bmatrix} \dfrac{-h_4}{k_3} & \dfrac{l_4}{k_3} \\ \dfrac{-m_4}{k_3} & \dfrac{k_4}{k_3} \end{bmatrix}. \qquad (4)$$

In this case, $\boldsymbol{E}_3/k_3$ and $\boldsymbol{E}_4/k_3$ are not consistent with $\boldsymbol{E}_1/k_1$ and $\boldsymbol{E}_2/k_1$ due to the different normalization term

$$\boldsymbol{E}_3/k_3 = \frac{k_1}{k_3} \boldsymbol{E}_3/k_1. \qquad (5)$$

The linking coefficient k_1/k_3 is still unknown.

---

[1]Multiline thru-reflect-line (TRL) [13] is preferred, but any two-port calibration is feasible, like short-open-load-thru (SOLT), TRL [14], line-reflect-match (LRM) [15] or short-open-load-reciprocal (SOLR) [16].
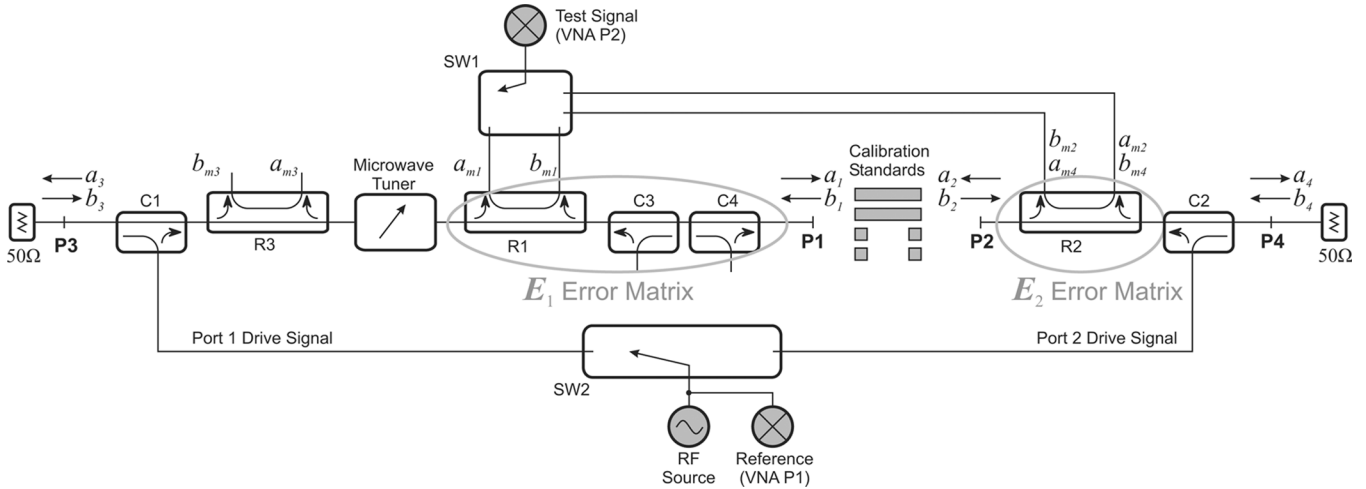
Fig. 5. Calibration at Ports 1 and 2. The schematic is a reduction of Fig. 1; for clarity, unused connections are not drawn.
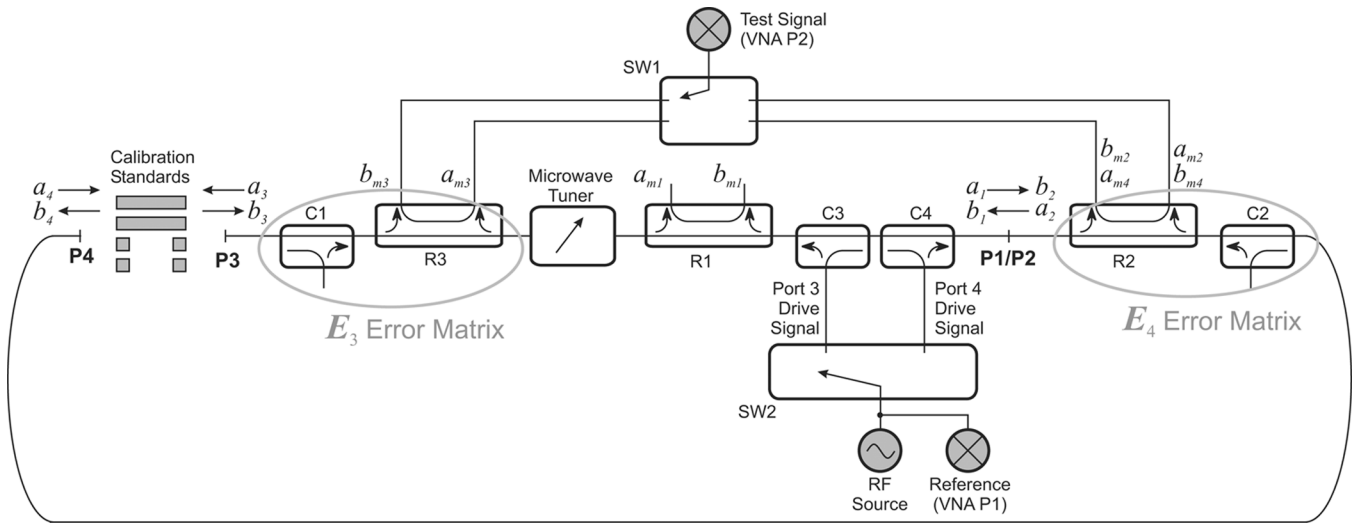

Fig. 6. Calibration at Ports 3 and 4. The schematic is a reduction of Fig. 1; for clarity, unused connections are not drawn.

Actually, a two-port calibration could be avoided in this step since it was anticipated that the P4 error coefficients are not used. A one-port short-open-load calibration could be performed as well at P3, giving $\boldsymbol{E}_3/k_3$, as well-established in load–pull techniques [17].

In this case, the P3 error coefficients would be affected by the greater uncertainties in the one-port standards definitions. The P1–P3 scattering parameters accuracy is paramount for the noise measurements, thus the system uses P4 as dummy port for an accurate two-port calibration such as the multiline TRL.

Step Three. The tuner section S-matrix from plane P3 to P1 is measured, and the P3 error coefficients are linked to the P1–P2 ones by a procedure similar to an unknown thru calibration [16]. The hardware model is sketched in Fig. 7, where two fictitious calibration planes (P5 and P6) represent the microwave tuner input and output ports.

The tuner alone is defined by the following transmission matrix:

Fig. 7. Calibration at Ports 1 and 3. The schematic is a reduction of Fig. 1; for clarity, unused connections are not drawn.

whereas two fictitious error matrices link the waves at the tuner ports with the measured quantities

$$\begin{bmatrix} b_5 \\ a_5 \end{bmatrix} = \boldsymbol{T}' \begin{bmatrix} a_6 \\ b_6 \end{bmatrix} \qquad (6)$$

$$\begin{bmatrix} a_5 \\ b_5 \end{bmatrix} = \boldsymbol{E}_5 \begin{bmatrix} a_{\mathrm{m5}} \\ b_{\mathrm{m5}} \end{bmatrix} \qquad \begin{bmatrix} a_6 \\ b_6 \end{bmatrix} = \boldsymbol{E}_6 \begin{bmatrix} a_{\mathrm{m6}} \\ b_{\mathrm{m6}} \end{bmatrix} \qquad (7)$$

being the measured waves

$$a_{m5} = b_{m3} \quad b_{m5} = a_{m3} \tag{8}$$
$$a_{m6} = b_{m1} \quad b_{m6} = a_{m1}. \tag{9}$$

From (6) and (7), the measured transmission matrix

$$\begin{bmatrix} b_{m5} \\ a_{m5} \end{bmatrix} = \boldsymbol{T}_m \begin{bmatrix} a_{m6} \\ b_{m6} \end{bmatrix} \tag{10}$$

is expressed as

$$\boldsymbol{T}_m = \boldsymbol{X}[\boldsymbol{E}_5]^{-1}\boldsymbol{X}\boldsymbol{T}'\boldsymbol{E}_6 \tag{11}$$

where $\boldsymbol{X} = \begin{bmatrix} 0 & 1 \\ 1 & 0 \end{bmatrix}$ is a 2×2 permutation matrix. This is analog to [16, eq. (4)], but in our case, $\boldsymbol{E}_5$ and $\boldsymbol{E}_6$ contain more than one unknown term, and thus, no solution can be found.

The calibration problem is solved by referencing the unknown error coefficients to the ones previously determined at P1 and P3, thus leading to an equation where only a single term (k_1/k_3) has to be determined. We define two transmission matrices $\boldsymbol{T}_1$ from plane P6 to P1, and $\boldsymbol{T}_3$ from P3 to P5

$$\begin{bmatrix} a_6 \\ b_6 \end{bmatrix} = \boldsymbol{T}_1 \begin{bmatrix} b_1 \\ a_1 \end{bmatrix} \quad \begin{bmatrix} a_3 \\ b_3 \end{bmatrix} = \boldsymbol{T}_3 \begin{bmatrix} b_5 \\ a_5 \end{bmatrix}. \tag{12}$$

$\boldsymbol{T}_1$ represents the cascade of R1, C3, and C4, while $\boldsymbol{T}_3$ the cascade of C1 and R3, which are all passive reciprocal devices.

In this way, from the error matrix definition (2), (7)–(9), and (12), $\boldsymbol{E}_5$ and $\boldsymbol{E}_6$ can be computed as

$$\boldsymbol{E}_5 = \boldsymbol{X}[\boldsymbol{T}_3]^{-1}\boldsymbol{E}_3\boldsymbol{X} \tag{13}$$
$$\boldsymbol{E}_6 = \boldsymbol{T}_1\boldsymbol{X}\boldsymbol{E}_1\boldsymbol{X} \tag{14}$$

and (11) is rewritten as

$$\boldsymbol{T}_m = \frac{k_1}{k_3}\left[\frac{\boldsymbol{E}_3}{k_3}\right]^{-1}\boldsymbol{T}_3\boldsymbol{T}'\boldsymbol{T}_1\boldsymbol{X}\left[\frac{\boldsymbol{E}_1}{k_1}\right]\boldsymbol{X}. \tag{15}$$

Finally, k_1/k_3 is computed from the determinant of $\boldsymbol{T}_m$, being the determinants of $\boldsymbol{T}_1$, $\boldsymbol{T}'$, and $\boldsymbol{T}_3$ unitary due to reciprocity

$$k_1/k_3 = \pm\sqrt{\frac{\det(\boldsymbol{T}_m)\det(\boldsymbol{E}_3/k_3)}{\det(\boldsymbol{E}_1/k_1)}} \tag{16}$$

and the sign ambiguity is solved by a prior knowledge of the electrical delay from plane P3 to P1. It is interesting to note that this step requires no additional standard connection.

B. Scattering Parameter Measurement

After completing all the calibration steps, it is possible to perform calibrated two-port measurement between the following.

• P1 and P2: the DUT S-parameters are measured by sampling the four readings a_{m1}, b_{m1}, a_{m2}, and b_{m2} for two different source drive signals (through couplers C1 and C2, respectively). The DUT S-matrix can be computed as

$$S = \left[\frac{\boldsymbol{B}}{k_1}\right]\left[\frac{\boldsymbol{A}}{k_1}\right]^{-1} \tag{17}$$

with

$$\frac{\boldsymbol{B}}{k_1} = -\begin{bmatrix} \frac{m_1}{k_1} & 0 \\ 0 & \frac{m_2}{k_1} \end{bmatrix}\boldsymbol{A}_m + \begin{bmatrix} 1 & 0 \\ 0 & \frac{k_2}{k_1} \end{bmatrix}\boldsymbol{B}_m \tag{18}$$

$$\frac{\boldsymbol{A}}{k_1} = -\begin{bmatrix} \frac{h_1}{k_1} & 0 \\ 0 & \frac{h_2}{k_1} \end{bmatrix}\boldsymbol{A}_m + \begin{bmatrix} \frac{l_1}{k_1} & 0 \\ 0 & \frac{l_2}{k_1} \end{bmatrix}\boldsymbol{B}_m \tag{19}$$

being the measured waves organized as

$$\boldsymbol{A}_m = \begin{bmatrix} a'_{m1} & a''_{m1} \\ a'_{m2} & a''_{m2} \end{bmatrix} \tag{20}$$

$$\boldsymbol{B}_m = \begin{bmatrix} b'_{m1} & b''_{m1} \\ b'_{m2} & b''_{m2} \end{bmatrix} \tag{21}$$

where the prime and double prime refer to the first and second RF source drive.

• P1 and P3: the S-parameters of the tuner section are computed from a_{m1}, b_{m1}, a_{m3}, and b_{m3} read in turn with the RF source driving in coupler C1 and C3. The same equations like (17)–(21) hold in this case: subscript 2 should be substituted with 3.

Several one-port reflection coefficients are also easily computed. When the RF drive is through C3, the noise source reflection coefficient at P3 (Γ_{src}) and the source reflection coefficient at plane P1 (Γ_S) are calculated as

$$\Gamma_{src} \equiv \left.\frac{b_3}{a_3}\right|_{C3} = \frac{\frac{k_3}{k_1}b_{m3} - \frac{m_3}{k_1}a_{m3}}{\frac{l_3}{k_1}b_{m3} - \frac{h_3}{k_1}a_{m3}} \tag{22}$$

$$\Gamma_S \equiv \left.\frac{a_1}{b_1}\right|_{C3} = \frac{\frac{l_1}{k_1}b_{m1} - \frac{h_1}{k_1}a_{m1}}{b_{m1} - \frac{m_1}{k_1}a_{m1}}. \tag{23}$$

The DUT output reflection coefficient can be measured driving from coupler C2 as

$$\Gamma_{out} \equiv \left.\frac{b_2}{a_2}\right|_{C2} = \frac{\frac{k_2}{k_1}b_{m2} - \frac{m_2}{k_1}a_{m2}}{\frac{l_2}{k_1}b_{m2} - \frac{h_2}{k_1}a_{m2}}. \tag{24}$$

Finally, the noise receiver input reflection coefficient, referenced to plane P2, is calculated as

$$\Gamma_{RX} \equiv \left.\frac{a_2}{b_2}\right|_{C4} = \frac{\frac{l_2}{k_1}b_{m2} - \frac{h_2}{k_1}a_{m2}}{\frac{k_2}{k_1}b_{m2} - \frac{m_2}{k_1}a_{m2}} \tag{25}$$

with a thru or low-loss device connected between P1 and P2 and RF drive through coupler C4.

IV. SYSTEM DESCRIPTION—NOISE PARAMETERS CAPABILITY

The presented system is based on an extension of the Y-factor technique, which computes the reading Y as the ratio of *hot* (P_H) and *cold* (P_C) received noise powers
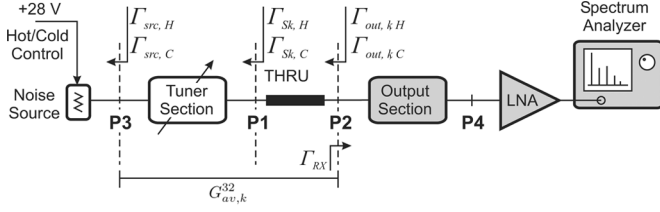
$$Y = \frac{P_H}{P_C}. \tag{26}$$

Fig. 8. Noise receiver calibration.

Fig. 9. DUT measurement model.

Since both powers depend on the receiver's gain, the gain instability effect is virtually eliminated, thus allowing us to use a commercial spectrum analyzer in place of more stable hardware. Moreover, we can adjust, for each measurement, the spectrum analyzer's IF gain in order to operate the logarithmic detector in its most linear range.

The receiver and DUT added noise are modeled by X-parameters, which were introduced in [18] and are of straightforward use with the noise-wave and scattering parameters formalism. Moreover, their computation is numerically stable [19]. A similar approach has recently been published in [20].

A. Noise Receiver Calibration Model

The noise receiver model is sketched in Fig. 8.

The receiver calibrated reference plane must be set at plane P2, i.e., directly at the DUT output. A thru or low-loss passive device is connected in place of the DUT.

In this way, the receiver is connected to an equivalent one-port source at P2. The source noise temperature $T_{\text{out},k,L}$ depends on the kth tuner position ($k = 1, \ldots, K$, being $K \geq 4$) and on the noise source state (hot $L = H$ or cold $L = C$). $T_{\text{out},k,L}$ is obtained from the P3–P2 section available gain $G_{\text{av},k}^{32}$ as (see Fig. 8)

$$T_{\text{out},k,L} = T_{\text{src},L} G_{\text{av},k}^{32}(\Gamma_{\text{src},L}) + T_{\text{amb}}\left(1 - G_{\text{av},k}^{32}(\Gamma_{\text{src},L})\right) \quad (27)$$

$$G_{\text{av},k}^{32}(\Gamma_{\text{src},L}) = \frac{|S_{23,k}|^2}{|1 - S_{33,k}\Gamma_{\text{src},L}|^2}\frac{1 - |\Gamma_{\text{src},L}|^2}{1 - |\Gamma_{\text{out},k,L}|^2} \quad (28)$$

where T_{amb} is the P3–P2 section's temperature, supposed uniform, $\Gamma_{\text{src},L}$ and $T_{\text{src},L}$ are the noise head reflection coefficient and noise temperature, respectively. $T_{\text{src},L}$ is known either from the ENR table (hot state) or from the physical temperature (cold state) [21]. $\Gamma_{\text{src},L}$ is measured using (22). The P3–P2 scattering parameters S_{22}, $S_{23} = S_{32}$, and S_{33} are computed by cascading the P3–P1 section and P1–P2 section measured scattering matrices from (17).

It is well known that the total measured noise power contains a contribution from the input termination, and one due to the receiver added noise

$$P_{k,L} = k_B \frac{B G_{RX}(1 - |\Gamma_{\text{out},k,L}|^2)}{|1 - \Gamma_{\text{out},k,L}\Gamma_{RX}|^2} \times [T_{\text{out},k,L} + T_{RX}(\Gamma_{\text{out},k,L})] \quad (29)$$

where B, G_{RX}, and Γ_{RX} are the receiver's bandwidth, gain, and input reflection coefficient, respectively. Γ_{RX} is measured with (25). T_{RX} is the receiver's equivalent noise temperature,
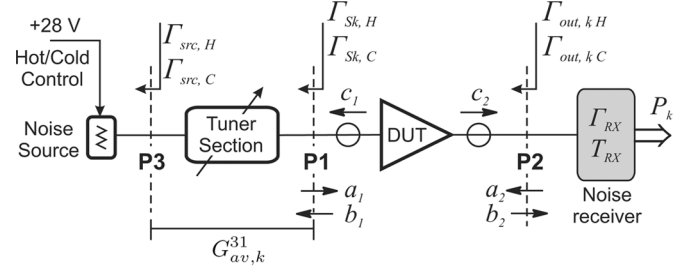
which is expressed in terms of X-parameters (from [22, eq. (5)]) as

$$T_{RX}(\Gamma_{\text{out},k,L}) = \frac{N_{RX}(\Gamma_{\text{out},k,L})}{1 - |\Gamma_{\text{out},k,L}|^2} \quad (30)$$

$$N_{RX}(\Gamma_{\text{out},k,L}) = |\Gamma_{\text{out},k,L}|^2 X_1 + 2\Re(\Gamma_{\text{out},k,L}(1 - \Gamma_{\text{out},k,L}^*\Gamma_{RX}^*)X_{12}) + |1 - \Gamma_{\text{out},k,L}\Gamma_{RX}|^2 X_2. \quad (31)$$

The Y-factor measurement becomes

$$Y_k = \frac{P_{k,H}}{P_{k,C}} = \frac{(1 - |\Gamma_{\text{out},k,H}|^2)\dfrac{T_{\text{out},k,H} + T_{RX}(\Gamma_{\text{out},k,H})}{|1 - \Gamma_{\text{out},k,H}\Gamma_{RX}|^2}}{(1 - |\Gamma_{\text{out},k,C}|^2)\dfrac{T_{\text{out},k,C} + T_{RX}(\Gamma_{\text{out},k,C})}{|1 - \Gamma_{\text{out},k,C}\Gamma_{RX}|^2}}. \quad (32)$$

If one could assume that the noise source reflection coefficient remains the same in the hot and cold states ($\Gamma_{\text{out},k,H} = \Gamma_{\text{out},k,C} = \Gamma_{\text{out},k}$), (32) would result in the usual form [23]

$$Y_k = \frac{T_{\text{out},k,H} + T_{RX}(\Gamma_{\text{out},k})}{T_{\text{out},k,C} + T_{RX}(\Gamma_{\text{out},k})}. \quad (33)$$

The calibration coefficients X_1, X_2, $\Re(X_{12})$, and $\Im(X_{12})$ are computed in the more general case from (32), as detailed in Appendix A.

B. DUT Noise Parameter Measurement

A two-port noise generating amplifier connected to P1 and P2 (Fig. 9) is modeled in terms of its scattering matrix and generated noise waves as [19]

$$\begin{bmatrix} b_1 \\ b_2 \end{bmatrix} = \begin{bmatrix} S_{11} & S_{12} \\ S_{21} & S_{22} \end{bmatrix}\begin{bmatrix} a_1 \\ a_2 \end{bmatrix} + \begin{bmatrix} c_1 \\ c_2 \end{bmatrix}. \quad (34)$$

The S-matrix is measured using (17).

The DUT noise sources are referenced to the input by the use of X-parameters

$$k_B X_1 = \overline{|c_1|^2} \quad (35)$$

$$k_B X_2 = \overline{|c_2/S_{21}|^2} \quad (36)$$

$$k_B X_{12} = \overline{c_1(c_2/S_{21})^*} \quad (37)$$

and the DUT output noise temperature becomes

$$T_{\text{out},k,L} = G_{\text{AV}}(\Gamma_{Sk,L})[T_{Sk,L} + T_{\text{DUT}}(\Gamma_{Sk,L})] \quad (38)$$

with $T_{Sk,L}$ and $\Gamma_{Sk,L}$ being the source reflection coefficient and noise temperature at plane P1, respectively. $\Gamma_{Sk,L}$ is directly measured using (23). The DUT equivalent noise temperature T_{DUT} and available gain G_{AV} are computed as

$$T_{\text{DUT}}(\Gamma_{Sk,L}) = \frac{N_{\text{DUT}}(\Gamma_{Sk,L})}{1 - |\Gamma_{Sk,L}|^2} \tag{39}$$

$$N_{\text{DUT}}(\Gamma_{Sk,L}) = |\Gamma_{Sk,L}|^2 X_1 + |1 - \Gamma_{Sk,L}S_{11}|^2 X_2 \\ + 2\Re(\Gamma_{Sk,L}(1 - \Gamma_{Sk,L}^* S_{11}^*)X_{12}) \tag{40}$$

$$G_{\text{AV}}(\Gamma_{Sk,L}) = \frac{|S_{21}|^2(1 - |\Gamma_{Sk,L}|^2)}{(1 - |\Gamma_{\text{out},k,L}|^2)|1 - S_{11}\Gamma_{Sk,L}|^2} \tag{41}$$

while $\Gamma_{\text{out},k,L}$ is directly measured using (24).

The source noise temperature $T_{Sk,L}$ in (38) is computed similarly to (27) using the tuner section measured losses from P3 to P1

$$T_{Sk,L} = T_{\text{src},L}G_{\text{av},k}^{31}(\Gamma_{\text{src},L}) + T_{\text{amb}}\left(1 - G_{\text{av},k}^{31}(\Gamma_{\text{src},L})\right) \tag{42}$$

where T_{amb} is the P3–P1 section's temperature and its available gain $G_{\text{av},k}^{31}$ is

$$G_{\text{av},k}^{31}(\Gamma_{\text{src},L}) = \frac{|S_{13,k}|^2}{|1 - S_{33,k}\Gamma_{\text{src},L}|^2}\frac{1 - |\Gamma_{\text{src},L}|^2}{1 - |\Gamma_{Sk,L}|^2}. \tag{43}$$

The Y-factor measurement is given by (32), which is rewritten using (38) and (41) as

$$Y_k\frac{|1 - \Gamma_{\text{out},k,H}\Gamma_{RX}|^2}{|1 - \Gamma_{\text{out},k,C}\Gamma_{RX}|^2} \\ = \frac{(1 - |\Gamma_{Sk,H}|^2)\dfrac{T'_{Sk,H} + T_{\text{DUT}}(\Gamma_{Sk,H})}{|1 - \Gamma_{Sk,H}S_{11}|^2}}{(1 - |\Gamma_{Sk,C}|^2)\dfrac{T'_{Sk,C} + T_{\text{DUT}}(\Gamma_{Sk,C})}{|1 - \Gamma_{Sk,C}S_{11}|^2}} \tag{44}$$

where

$$T'_{Sk,L} = T_{Sk,L} + \frac{T_{RX}(\Gamma_{\text{out},k,L})}{G_{\text{AV}}(\Gamma_{Sk,L})}. \tag{45}$$

and T_{RX} is known from the noise receiver calibration.

Equation (44) is used to compute the DUT X-parameters, as shown in Appendix A. The usual noise parameters (minimum noise temperature T_{min}, optimum reflection coefficient Γ_{opt}, and noise resistance R_n) can be computed by the formulas given in Appendix B.

V. MEASUREMENT RESULTS

We initially checked the scattering parameter capability comparing the measured results of the presented system with those from an independent VNA (HP8510A). Multiline TRL calibrations were performed between planes P1–P2 and P3–P4 and at the independent VNA. All the connectors were 7-mm connectors, and we used the same standards (APC7 short, 10- and 20-cm airlines) for all calibrations.

The first measured device was a 10-dB APC7 attenuator. The measurement was made at planes P1–P2 on the proposed test-set and with the auxiliary VNA. The magnitude and phase differences of the S_{21}-parameter are plotted in Fig. 10.
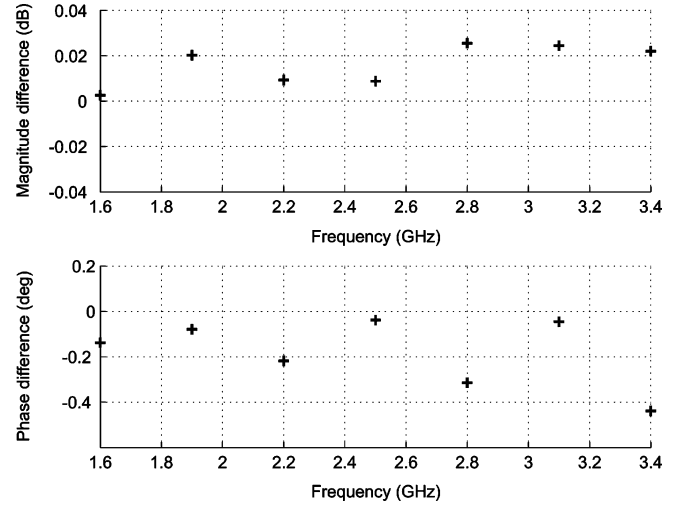

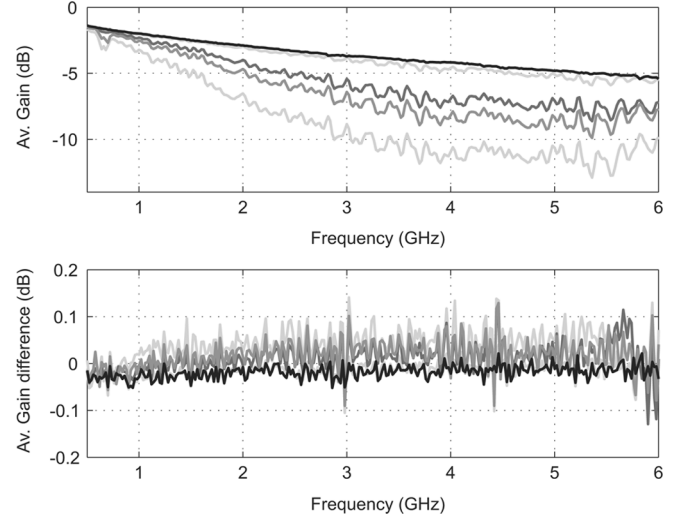Fig. 10. Measured difference of the 10-dB attenuator's S_{21} parameter.

Fig. 11. Available gain comparison for five different tuner positions. The P3 reflection coefficient used is the measured hot reflection coefficient of the noise source.

The second measured device was the system's tuner section from plane P3 to P1 (Fig. 1). The computed available gain is reported in Fig. 11 for five different tuner positions.

The biggest differences near 1.5, 3, 4.5, and 6 GHz are due to the poor phase margin of the standard sequence used in the multiline TRL calibrations, as at these frequencies the airlines' phase shifts approach 0° or 180°.

We then checked the noise figure capability by a comparison based on 50-Ω noise-figure measurements of a Mini-Circuits ZX60-6013E+ broadband amplifier. The DUT noise parameters were extracted twice, in two consecutive days, and the respective 50-Ω noise figures were computed. An independent measurement performed with a 50-Ω noise system (Anritsu MS4623B) was used as reference. In all these measurements, the noise head was the same (Noise/COM NC346B). The results are plotted in Fig. 12, showing good agreement.

Finally, the accuracy of the extracted optimum reflection coefficient Γ_{opt} and noise resistance R_n was assessed. We mimicked the behavior of a transistor by a cascade made of a manual
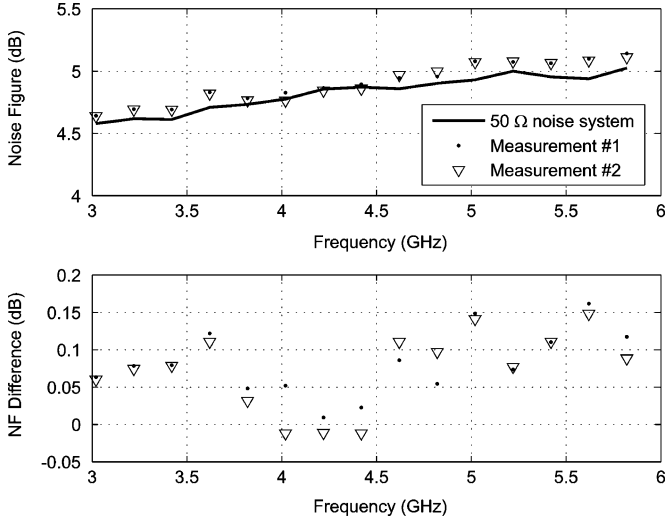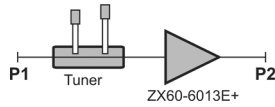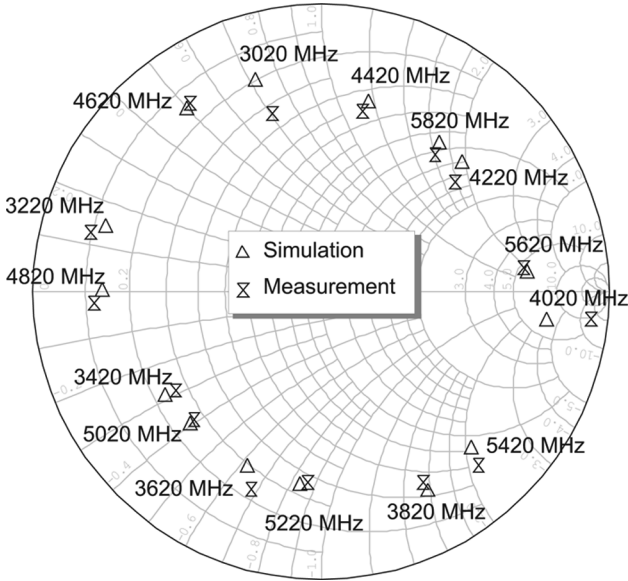
Fig. 12. 50-Ω noise-figure comparison.

Fig. 13. DUT used in the Γ_{opt} and R_n test.

Fig. 14. Optimum reflection coefficient Γ_{opt} versus frequency of the system in Fig. 13.

passive double-slug tuner fixed to high reflection and the amplifier used in the previous test (Fig. 13). The extracted noise parameters of the amplifier alone, and the measured tuner S-parameters were used in a circuit simulator. The measured noise parameters of the cascade were then compared with the simulated ones. The results are shown in Figs. 14 and 15, respectively.
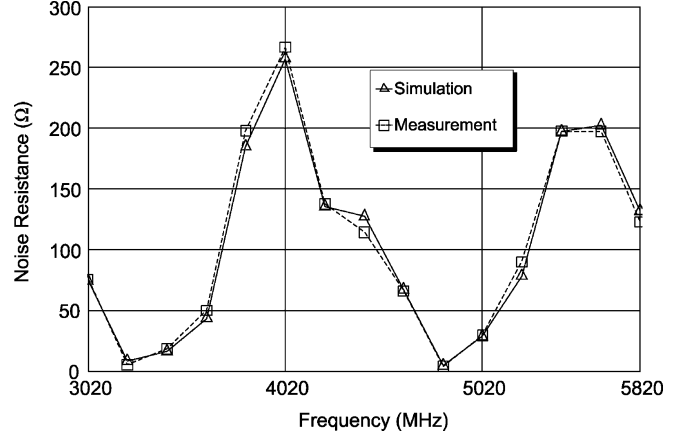
Fig. 15. Noise resistance R_n versus frequency of the system in Fig. 13.

VI. CONCLUSION

We presented an innovative scattering- and noise-parameter test-set. The system advantage relies on the accurate measurement of the losses between the noise head and the DUT input. An original multiport calibration scheme was studied to avoid the use of electromechanical switches along the noise signal path.

The measurements show the reliability and accuracy of the presented test-set.

Improvements in accuracy, especially for highly mismatched devices, are expected by reducing the losses with ultra-low-loss directional couplers in the test-set [24].

APPENDIX A
NOISE PARAMETER FITTING

Both (32) and (44) can be written in the form

$$Y_k' = \frac{(1-|\Gamma_{k,H}'|^2)\dfrac{T_{k,H}' + T_e(\Gamma_{k,H}')}{|1-\Gamma_{k,H}'\Gamma_e|^2}}{(1-|\Gamma_{k,C}'|^2)\dfrac{T_{k,C}' + T_e(\Gamma_{k,C}')}{|1-\Gamma_{k,C}'\Gamma_e|^2}}. \quad (46)$$

During the noise receiver calibration (32), the following is used: $Y_k' = Y_k$, $\Gamma_{k,L}' = \Gamma_{\text{out},k,L}$, $T_{k,L}' = T_{\text{out},k,L}$, $T_e = T_{RX}$, and $\Gamma_e = \Gamma_{RX}$.

For the DUT measurement (44), the following holds: $Y_k' = Y_k(|1-\Gamma_{\text{out},k,H}\Gamma_{RX}|^2)/(|1-\Gamma_{\text{out},k,C}\Gamma_{RX}|^2)$, $\Gamma_{k,L}' = \Gamma_{Sk,L}$, $T_{k,L}' = T_{Sk,L}'$, $T_e = T_{\text{DUT}}$, and $\Gamma_e = S_{11}$, where S_{11} is the DUT S-parameter.

T_e is a function of the X-parameters as

$$T_e(\Gamma_{k,L}') = \frac{N_e(\Gamma_{k,L}')}{1-|\Gamma_{k,L}'|^2} \quad (47)$$

$$N_e(\Gamma_{k,L}') = |\Gamma_{k,L}'|^2 X_1 + |1-\Gamma_{k,L}'\Gamma_e|^2 X_2 \\ + 2\Re(\Gamma_{k,L}'(1-\Gamma_{k,L}'^*\Gamma_e^*)X_{12}). \quad (48)$$

Thus, a linear system with the X-parameters as unknowns is derived from (46); each system row looks like

$$\begin{bmatrix} A_k & B_k & C_k & D_k \end{bmatrix} \begin{bmatrix} X_1 \\ X_2 \\ \Re(X_{12}) \\ \Im(X_{12}) \end{bmatrix} = M_k \qquad (49)$$

where

$$A_k = Y_k \frac{|\Gamma'_{k,C}|^2}{|1 - \Gamma'_{k,C}\Gamma_e|^2} - \frac{|\Gamma'_{k,H}|^2}{|1 - \Gamma'_{k,H}\Gamma_e|^2} \qquad (50)$$

$$B_k = Y_k - 1 \qquad (51)$$

$$C_k = 2\Re\left(Y_k \frac{\Gamma'_{k,C}}{1 - \Gamma'_{k,C}\Gamma_e} - \frac{\Gamma'_{k,H}}{1 - \Gamma'_{k,H}\Gamma_e}\right) \qquad (52)$$

$$D_k = -2\Im\left(Y_k \frac{\Gamma'_{k,C}}{1 - \Gamma'_{k,C}\Gamma_e} - \frac{\Gamma'_{k,H}}{1 - \Gamma'_{k,H}\Gamma_e}\right) \qquad (53)$$

$$M_k = \frac{T'_{k,H}(1 - |\Gamma'_{k,H}|^2)}{|1 - \Gamma'_{k,H}\Gamma_e|^2} - Y_k \frac{T'_{k,C}(1 - |\Gamma'_{k,C}|^2)}{|1 - \Gamma'_{k,C}\Gamma_e|^2}. \qquad (54)$$

Typically, an accurate solution is found in the least squares sense, with the number of tuner positions greater than four.

APPENDIX B
X-PARAMETERS TO IEEE NOISE PARAMETERS

The relationships between X-parameters and standard IEEE noise parameters $(T_{\min}, \Gamma_{\mathrm{opt}}, R_n)$ were published in [25], and are reproduced here for convenience.

The DUT equivalent temperature is expressed as

$$T_e(\Gamma) = T_{\min} + t \frac{|\Gamma_{\mathrm{opt}} - \Gamma|^2}{|1 + \Gamma_{\mathrm{opt}}|^2(1 - |\Gamma|^2)} \qquad (55)$$

where Γ is the source reflection coefficient, $t = (4T_0 R_n)/(Z_0)$, with $T_0 = 290$ K and Z_0 being the reference impedance (usually 50 Ω), and

$$t = X_1 + |1 + S_{11}|^2 X_2 - 2\Re(X_{12}(1 + S_{11})^*) \qquad (56)$$

$$T_{\min} = \frac{X_2 - |\Gamma_{\mathrm{opt}}|^2 \left[X_1 + |S_{11}|^2 X_2 - 2\Re(S_{11}^* X_{12})\right]}{1 + |\Gamma_{\mathrm{opt}}|^2} \qquad (57)$$

$$\Gamma_{\mathrm{opt}} = \frac{\eta}{2}\left(1 - \sqrt{1 - \frac{4}{|\eta|^2}}\right) \qquad (58)$$

$$\eta = \frac{X_2(1 + |S_{11}|^2) + X_1 - 2\Re(S_{11}^* X_{12})}{X_2 S_{11} - X_{12}}. \qquad (59)$$

ACKNOWLEDGMENT

REFERENCES

[1] H. A. Haus, W. R. Atkinson, G. M. Branch, W. B. Davenport, W. H. Fonger, W. A. Harris, W. W. McLeod, and E. K. Stodola, "IRE standards on methods of measuring noise in linear twoports, 1959," *Proc. IRE*, vol. 48, no. 1, pp. 60–68, Jan. 1960.

[2] A. Davidson, B. Leake, and E. Strid, "Accuracy improvements in microwave noise parameter measurements," *IEEE Trans. Microw. Theory Tech.*, vol. MTT-37, no. 12, pp. 1973–1978, Dec. 1979.

[3] M. H. Weatherspoon, L. P. Dunleavy, A. Boudiaf, and J. Randa, "Vector corrected noise temperature measurements," in *IEEE MTT-S Int. Microw. Symp. Dig.*, Seattle, WA, Jun. 2–7, 2002, vol. 3, pp. 2253–2256.

[4] L. Escotte, F. Sejalon, and J. Graffeuil, "Noise parameter measurement of microwave transistors at cryogenic temperature," *IEEE Trans. Instrum. Meas.*, vol. 43, no. 4, pp. 536–543, Aug. 1994.

[5] M. Sannino, "On the determination of device noise and gain parameters," *Proc. IEEE*, vol. 67, no. 9, pp. 1364–1366, Sep. 1979.

[6] M. Sannino, "Simultaneous determination of device noise and gain parameters through noise measurements only," *Proc. IEEE*, vol. 68, no. 10, pp. 1343–1345, Oct. 1980.

[7] H. T. Friis, "Noise figures of radio receivers," *Proc. IRE*, vol. 32, no. 7, pp. 419–422, Jul. 1944.

[8] "MT993-2 Operating Manual," Maury Microw., Ontario, CA, 2002.

[9] "Product Catalogue," Focus Microw., Dollard-des-Ormeaux, QC, Canada, 2008.

[10] L. F. Tiemeijer, R. J. Havens, R. de Kort, and A. J. Scholten, "Improved Y-factor method for wide-band on-wafer noise-parameter measurements," *IEEE Trans. Microw. Theory Tech.*, vol. 53, no. 9, pp. 2917–2925, Sep. 2005.

[11] A. Ferrero, V. Teppati, M. Garelli, and A. Neri, "A novel calibration algorithm for a special class of multiport vector network analyzers," *IEEE Trans. Microw. Theory Tech.*, vol. 56, no. 3, pp. 693–699, Mar. 2008.

[12] H. J. Eul and B. Schiek, "Thru-match-reflect: One result of a rigorous theory for de-embedding and network analyzer calibration," in *18th Eur. Microw. Conf.*, Oct. 1988, pp. 909–914.

[13] R. B. Marks, "A multiline method of network analyzer calibration," *IEEE Trans. Microw. Theory Tech.*, vol. 39, no. 7, pp. 1205–1215, Jul. 1991.

[14] G. F. Engen and C. A. Hoer, "Thru-reflect-line: An improved technique for calibrating the dual six-port automatic network analyzer," *IEEE Trans. Microw. Theory Tech.*, vol. MTT-27, no. 12, pp. 987–993, Dec. 1979.

[15] H. J. Eul and B. Schiek, "A generalized theory and new calibration procedures for network analyzer self-calibration," *IEEE Trans. Microw. Theory Tech.*, vol. 39, no. 4, pp. 724–731, Apr. 1991.

[16] A. Ferrero and U. Pisani, "Two-port network analyzer calibration using an unknown 'thru'," *IEEE Microw. Guided Wave Lett.*, vol. 2, no. 12, pp. 505–507, Dec. 1992.

[17] A. Ferrero and U. Pisani, "An improved calibration technique for on-wafer large-signal transistor characterization," *IEEE Trans. Instrum. Meas.*, vol. 47, no. 2, pp. 360–364, Apr. 1993.

[18] J. Randa, "Noise-parameters uncertainties: A Monte Carlo simulation," *J. Res. Nat. Inst. Stand. Technol.*, vol. 107, no. 5, pp. 431–444, Sep. 2002.

[19] S. W. Wedge and D. B. Rutledge, "Wave techniques for noise modeling and measurement," *IEEE Trans. Microw. Theory Tech.*, vol. 40, no. 11, pp. 2004–2012, Nov. 1992.

[20] D. Pasquet, E. Bourdel, S. Quintanel, T. Ravalet, and P. Houssin, "New method for noise-parameter measurement of a mismatched linear twoport using noise power wave formalism," *IEEE Trans. Microw. Theory Tech.*, vol. 56, no. 9, pp. 2136–2142, Sep. 2008.

[21] H. Bosma, "On the theory of linear noisy systems," *Philips Res. Rep. Suppl.*, no. 10, pp. 1–190, 1967.

[22] J. Randa and D. K. Walker, "On-wafer measurement of transistor noise parameters at NIST," *IEEE Trans. Instrum. Meas.*, vol. 56, no. 2, pp. 551–554, Apr. 2007.

[23] G. Caruso and M. Sannino, "Analysis of frequency-conversion techniques in measurements of microwave transistor noise temperatures," *IEEE Trans. Microw. Theory Tech.*, vol. MTT-25, no. 11, pp. 870–873, Nov. 1977.

[24] V. Teppati and A. Ferrero, "A new class of nonuniform, broadband, nonsymmetrical rectangular coaxial-to-microstrip directional couplers for high power applications," *IEEE Microw. Wireless Compon. Lett.*, vol. 13, no. 4, pp. 152–154, Apr. 2003.

[25] J. Randa and W. Wiatr, "Monte Carlo estimation of noise-parameter uncertainties," *Proc. Inst. Elect. Eng.—Sci. Meas. Technol.*, vol. 149, no. 6, pp. 333–337, Nov. 2002.

Andrea Ferrero (S'85–M'85–SM'06) was born in Novara, Italy, on November 7, 1962. He received the Laurea degree in electronic engineering and Ph.D. degree in electronics from the Politecnico di Torino, Turin, Italy, in 1987 and 1992, respectively.

In 1988, he joined the Aeritalia Company, as a Microwave Consultant. In 1991, he was with the Microwave Technology Division, Hewlett-Packard Company, Santa Rosa, CA, as a Summer Student. In 1995, he was with the Department of Electrical Engineering, Ecole Polytechnique de Montréal, Montréal, QC, Canada, as a Guest Researcher. He became an Associate and Full Professor of electronic measurements with the Department of Electronics, Politecnico di Torino, in 1998 and 2006, respectively. His main research activities are in the areas of microwave measurement techniques, calibration, and modeling.

Dr. Ferrero was the recipient of the 2006 Automatic RF Techniques Group Technology Award for the development and implementation of VNA calibration algorithms and nonlinear measurement techniques.

Marco Garelli (S'04–M'09) was born in Cuneo, Italy, in 1981. He received the Electronic Engineering degree from the Politecnico di Torino, Turin, Italy, in 2005, and is currently working toward the Ph.D. degree in metrology at the Politecnico di Torino.

During 2007 and 2008, he was with the National Institute of Standards and Technology (NIST), Boulder, CO, as a Guest Researcher involved with material and noise projects. His main interests are in the area of RF and microwave measurement techniques.

Serena Bonino was born in Cuneo, Italy, in 1983. She received the Master of Science degree in computer science and electrical engineering from the University of Illinois at Chicago, Chicago, in 2007, the Electronic Engineering degree from the Politecnico di Torino, Turin, Italy, in 2007 , and is currently working toward the Ph.D. degree in metrology from the Politecnico di Torino.

Her reseach efforts are mainly focused on RF and microwave measurement techniques.